JOC The Journal of Organic Chemistry

Article

pubs.acs.org/joc

FormylBODIPYs: Privileged Building Blocks for Multicomponent Reactions. The Case of the Passerini Reaction

Diana E. Ramírez-Ornelas,[†] Enrique Alvarado-Martínez,[†] Jorge Bañuelos,*[,‡] Iñigo López Arbeloa,[‡] Teresa Arbeloa,[‡] Héctor M. Mora-Montes,[§] Luis A. Pérez-García,[§] and Eduardo Peña-Cabrera*[,†]

[†]Departamento de Química and [§]Departamento de Biología, Universidad de Guanajuato, Col. Noria Alta S/N, Guanajuato 36050, Mexico

[‡]Departamento de Química Física, Universidad del País Vasco-EHU, Apartado 644, 48080 Bilbao, Spain

Supporting Information

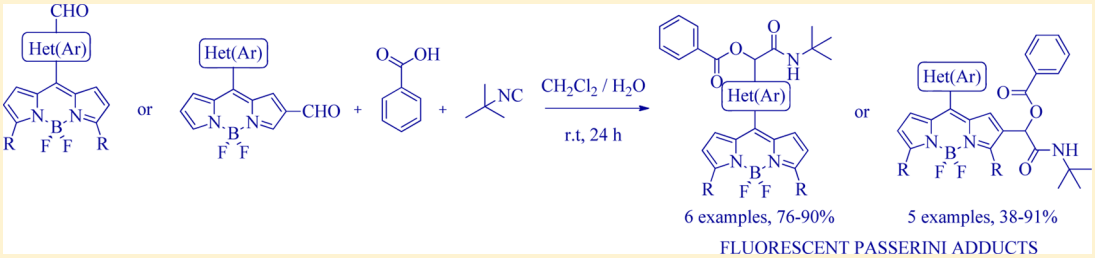

ABSTRACT: Eleven formyl-containing BODIPY dyes were prepared by means of either the Liebeskind−Srogl cross-coupling reaction or the Vilsmeier reaction. These dyes were used as components in the Passerini reaction to give highly substituted BODIPY dyes. A joined spectroscopic and theoretical characterization of the synthesized compounds was conducted to unravel the impact of the structural rigidity/flexibility on the photophysical signatures. These dyes were tested as fluorescent trackers for phagocytosis. Additionally, they proved to be useful to stain different blood cells with an intense and stable signal at a very low exposure time.

INTRODUCTION

Multicomponent reactions (MCR) are ideal processes to generate chemical complexity in an efficient and atom-economical way.[1] Several applications of these reactions can be found in the literature. For example, they have been used to prepare nitrogen-enriched heterocyclic scaffolds,[2] imidazo-[1,2-*a*]pyridines,[3] dihydropyrroles,[4] substituted 1*H*-chromeno-[2,3-*d*]pyrimidine-5-carboxamides,[5] imidazoles,[6] amino acids,[7] 1,4-benzodiazepine-2,5-diones,[8] and N-substituted diketopiperazines,[9] just to mention a few. It is clear that in the majority of the examples reported, aldehydes play a crucial role, and therefore, it is of paramount importance to be able to prepare the aldehyde component for the specific sought after application. Many of the complex structures that are constructed after MCRs possess important properties, such as cytotoxic activity against the human lung cancer cell line,[10] antimicrobial and antioxidant,[11] aggregation-induced emitters,[12] and antitumor agents.[13] An additional property that would be highly desirable for the MCR adducts to have is fluorescence. This property would provide plenty of information about processes that take place on and inside cells.[14] Some groups have devoted considerable efforts to prepare fluorescent molecules using MCR. For instance, Wang et al. prepared polysubstituted 2,6-dicyanoanilines and iminocumarins.[15] Balakirev and co-workers developed fluorescent pharmacophores in droplet arrays.[16] Müller and collaborators prepared fluorescent indolizines.[17] In a pioneering paper, Vendrell, Lavilla, and co-workers reported several isonitrile-based MCRs to prepare fluorescent probes for in vivo imaging of phagocytic macrophages.[18] They chose to use a BODIPY[19] (borondipyrromethene)-containing isonitrile **1**, to carry out a Passerini,[20] a Bienaymé−Blackburn−Groebcke,[21] and variants of the Ugi reaction.[22]

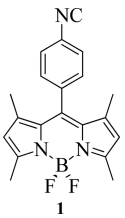

1

Despite the fact that such work was a ground-breaking contribution, no variation of the functional groups in **1** was presented. In that regard, another good candidate for MCRs, where the final product would be fluorescent (FMCR), is a formyl-containing BODIPY of the type **2** or **3** (Figure 1).

RESULTS AND DISCUSSION

Our laboratory has devised a versatile method to prepare, in a very straightforward way, a series of *meso*-formylhet(aryl)BODIPYs using the Liebeskind−Srogl coupling reaction starting from

Received: January 25, 2016
Published: March 11, 2016

DOI: 10.1021/acs.joc.5b02893
J. Org. Chem. 2016, 81, 2888−2898

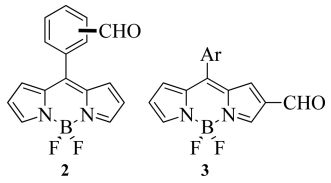

Figure 1. Formyl-containing BODIPYs suitable for FMCR.

Scheme 1. Application of the Liebeskind−Srogl Coupling in the Synthesis of *meso*-Formylhet(aryl)BODIPYs from the Biellmann BODIPYs A−C

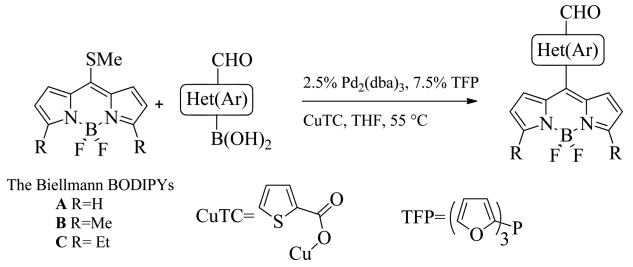

commercially available Biellmann BODIPYs **A**−**C**[23] (Scheme 1).[24] In those contributions, we underscore the fact that, with this methodology, the preparation of formyl-containing BODIPYs becomes trivial, and one does not have to face the regioselectivity issues posed by the typical Lindsey methodology that entails the condensations of a benzaldehyde with pyrrole under acidic conditions.

The synthesis of 2-formylBODIPYs is well-documented in the literature.[25] In this contribution, we demonstrate the applicability of several highly functionalized formyl-containing BODIPYs in the Passerini reaction.

FormylBODIPYs of the type **2** were prepared according to Scheme 1, and the results are shown in Scheme 2.

Scheme 2. Synthesized FormylBODIPYs of Type 2[a]

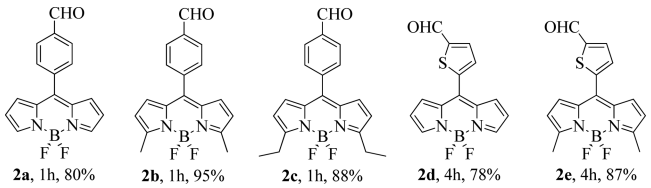

2a, 1h, 80% **2b**, 1h, 95% **2c**, 1h, 88% **2d**, 4h, 78% **2e**, 4h, 87%

[a]Conditions: Biellmann BODIPY (1 equiv), formylboronic acid (3 equiv), $Pd_2(dba)_3$ (2.5%), TFP (7.5%), CuTC (3 equiv), THF, 55 °C.

A more functionalized formylBODIPY **2f** was prepared according to Scheme 3 using our recently reported orthogonal reactivity of BODIPY **D**.[26]

BODIPYs of the type **3** were prepared according to the reported method (Scheme 4).

FormylBODIPYs **2a**−**f** and **3a**−**e** were utilized as components in the Passerini reaction along with benzoic acid and *t*-butyl isonitrile. The results are illustrated in Scheme 5.

In general, the reaction is operationally simple. In all cases, except for **5b**, the reaction went to completion in 24 h. A general trend was observed; the yields were higher when the formyl group was located on the 8-het(aryl) ring (compounds **4a**−**f**). When the formyl group was connected directly to the BODIPY core, the yields were lower (except for **5b**), presumably because of a diminished electrophilicity of the aldehyde group due to the electron-releasing properties of the BODIPY unit at position 2 (Figure 2).

Additionally, substituents on the *meso*-aryl group of 2-formylBODIPYs also affected the chemical yield. When the *meso*-aryl ring contained electron-withdrawing groups, the yields dropped (**5c** and **5d**).

Spectroscopical Properties. The photophysical signatures of those BODIPYs resulting from the MCR (**4a**−**f** and **5a**−**e**, Scheme 5) are summarized in Table 1. Overall, the absorption properties of the BODIPY are hardly affected by the 8-arylation, due to the low resonance interaction between their electronic clouds, at least in the ground state. Indeed, the computing molecular orbitals (see HOMO of **5a**,**b** in Figure 3) predict almost no extension of the delocalized π-system from the indacene core to the *meso*-aryl fragment. However, the fluorescence response of the BODIPYs bearing an unhindered 8-phenyl (**4a** and **5a**) is rather low (lower than 4% with a lifetime of hundred of picoseconds) due to a remarkable high internal conversion probability caused by the free rotational motion of such a ring (energy barrier around 12 kcal/mol in Figure 4).[24b,1] Moreover, the LUMO of **5a** places electronic density at the 8-aryl upon excitation (Figure 3), suggesting more degree of electronic coupling with the BODIPY, which eventually could lead to a strong interaction and cause a severe distortion of the chromophore planarity (Figure 4).[27] Indeed, such nonradiative pathways are fully suppressed when the aryl is locked in an orthogonal arrangement by methylation at its *ortho* positions (**5b**). The high rotational barrier of the mesityl group (around 45 kcal/mol) disables the free motion of the aryl, and the bright fluorescence efficiency characteristic of BODIPYs is recovered (82% with long lifetimes, 6.5 ns in Table 1).[28] Accordingly, the contribution of the aryl to the LUMO orbital is almost negligible because the electronic coupling is hampered.

The simple alkylation at the α positions (3 and 5) of pyrroles (see **4b** and **4c** vs **4a** in Scheme 5) leads to a bathochromic shift of the spectral bands and a slight increase of both the absorption probability (with values up to 82 400 M^{-1} cm^{-1}) and the fluorescence efficiency (Figure 5), which is ascribed to a more planar structure and thereby a more aromatic chromophore.[29] Whereas the *para*-functionalization of the 8-phenyl (bromine **5c** and trifluoromethyl **5d**) does not alter the photophysics of the BODIPYs (being identical to the **5a** counterpart, Scheme 5),

Scheme 3. Synthesis of BODIPY 2f

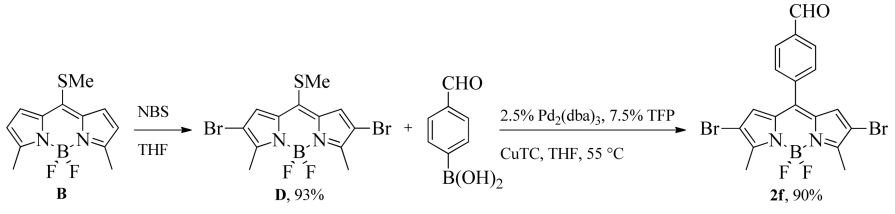

B **D**, 93% **2f**, 90%

DOI: 10.1021/acs.joc.5b02893
J. Org. Chem. 2016, 81, 2888−2898

Scheme 4. Synthesis of 8-(Het)aryl-2-formylBODIPYs[a,b]

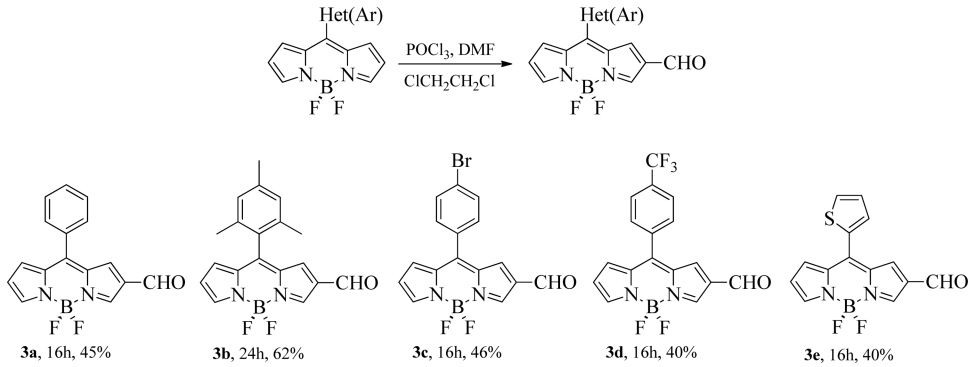

[a]Isolated yields. [b]Conditions: (1) BODIPY (1 equiv), $POCl_3$/DMF (160 equiv), DCE (10 mL), 80 °C; (2) saturated aq K_2CO_3, 1 h.

Scheme 5. Synthesis of the Passerini BODIPY Adducts[a]

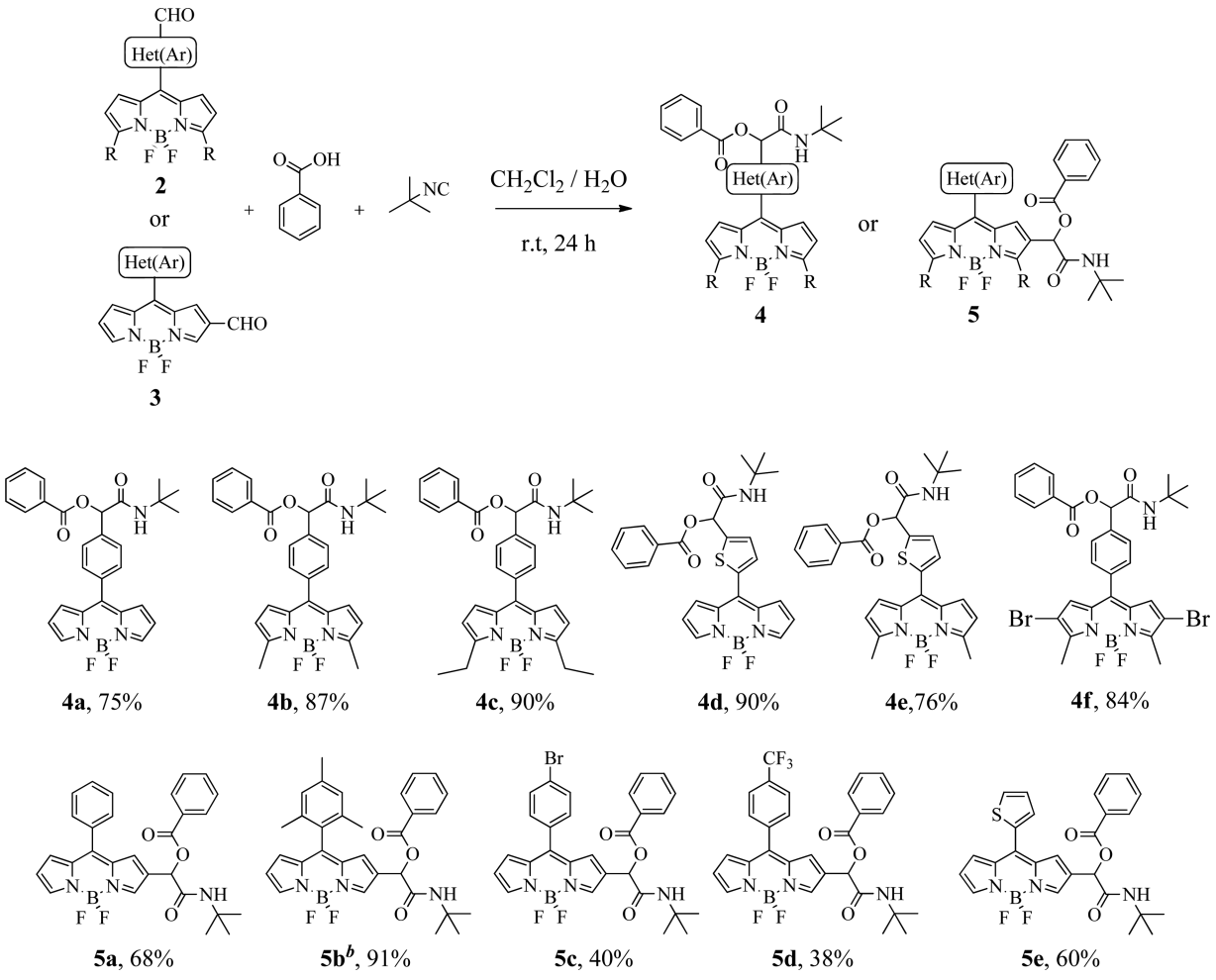

[a]Isolated yields. Conditions: formylBODIPY (1 equiv), benzoic acid (3 equiv), *tert*-butyl isocyanide (3 equiv), CH_2Cl_2/H_2O (1:1, 1 mL), rt. [b]The reaction took 48 h for this substrate.

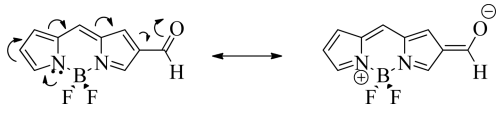

Figure 2. Decreased electrophilicity of the formyl group at position 2.

the β-bromination (positions 2 and 6) effect is noteworthy (**4f**, Figure 5). As a common rule, this heavy atom shifts the spectral bands bathochromically and increases the intersystem crossing.[30] As a consequence, the direct linkage of the bromine heteroatom usually quenches the fluorescence deactivation of the BODIPY. However, in the BODIPYs with unlocked 8-rings, the bromination provides improved fluorescence efficiencies (from 4% in **4b** to 25% with a lifetime of 2.45 ns, Table 1). Thus, the deleterious effect of the aryl-free motion can be counteracted not only by steric hindrance but also with

DOI: 10.1021/acs.joc.5b02893
J. Org. Chem. 2016, 81, 2888−2898

Table 1. Photophysical Properties of the Resulting BODIPY Derivatives after MCR (4a–f and 5a–e, Scheme 5) from the Corresponding Formylated Dyes in Ethyl Acetate

	λ_{ab}[a] (nm)	ε_{max}[b] ($\times10^{-4}$, M^{-1} cm^{-1})	λ_{fl}[c] (nm)	ϕ[d]	τ[e] (ns)	k_f[f] ($\times10^{-7}$, s^{-1})	k_{nr}[g] ($\times10^{-9}$, s^{-1})
4a	499.5	5.8	518.0	0.01	0.20	9.62	7.6
4b	509.5	8.2	525.0	0.04	1.05	3.81	0.9
4c	510.5	7.3	526.0	0.04	0.93	4.30	1.0
4d[h]	509.5	4.6	530.0		0.09(68%)–0.56(32%)		
			657.0		0.30		
4e[h]	520.5	5.9	549.0		0.15(75%)–0.37(25%)		
			645.0		0.35		
4f	540.0	7.5	561.0	0.25	2.45	10.2	0.3
5a	505.0	4.7	525.5	0.03	0.34	10.0	2.8
5b	505.5	6.6	522.0	0.82	6.51	12.6	0.03
5c	507.0	5.1	529.5	0.02	0.24	8.33	4.1
5d	509.5	5.1	530.5	0.02	0.21	9.52	4.7
5e[h]	513.5	4.1	549.0		0.18(70%)–0.47(30%)		
			646.0		0.50		

[a]Absorption wavelength. [b]Molar absorption. [c]Fluorescence wavelength. [d]Fluorescence quantum yield. [e]Lifetime. [f]Radiative deactivation rate constants. [g]Nonradiative deactivation rate constants. [h]In the BODIPYs bearing and an 8-thienyl fragment (**4d,e** and **5e**), the fluorescence quantum yield is not given because two overlapped emission bands are detected simultaneously.

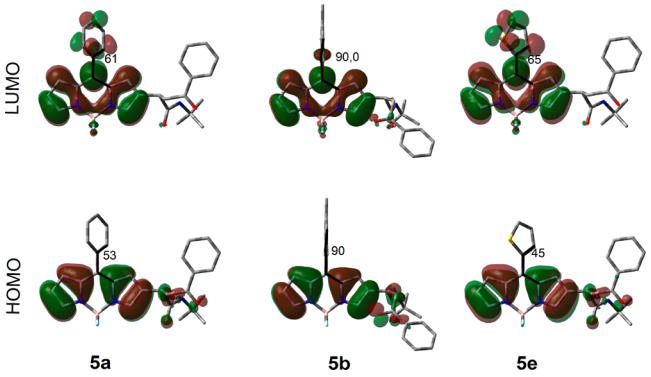

Figure 3. Computed frontier molecular orbitals for the representative compounds **5a,b** and **5e**. The corresponding dihedral angles between the indacene and the aryl planes from the optimized ground and excited state geometries are also included.

electronegative atoms that remove electronic density from the *meso* position.[31]

The presence of the thienyl group at the *meso* position (**4d,e** and **5e**) does not affect the position of the absorption band (Table 1), confirming again the absence of electronic coupling of aromatic rings at such positions in the ground state (Figure 3). It should be noticed that thiophene leads to effective resonance interactions to develop red-emitting BODIPYs but at position α or β of the chromophoric core or even fused to it.[32] However, its high electron-releasing ability in the highly sensitive *meso* position induces significant changes in the emission spectrum (Figure 6). The fluorescence signal from the locally excited (LE) state of the BODIPY (530–550 nm) is drastically quenched, and a new broad band appears at 645–655 nm, which is ascribed to the population of an intramolecular charge transfer state (ICT) from the donor thienyl group to the acceptor BODIPY.[33] The intensity of this new emission markedly changes with the solvent polarity. Thus, it decreases progressively as the solvent polarity is increased. In these media, the charge separation is further stabilized (low probability of charge recombination) and the nonradiative deactivation from the ICT prevails over the radiative one.[34] As a consequence, in the more polar solvent, the fluorescence signal is hardly detected. As a matter of fact, note that the additional presence of the inductive donor methyl groups at α positions (**4e**) leads to an emission from the ICT less intense than that from the LE, owing to the higher stabilization of the ICT state claimed above, whereas in **4d** (non-alkylated chromophore), the ICT band is more intense than the emission from the LE state (Figure 6). It is remarkable that this solvent-switchable new emission depends on the geometrical arrangement of the thienyl fragment because, when it is disposed fully orthogonal (by the steric hindrance at the adjacent positions 1 and 7) with regard to the BODIPY core, the ICT is also operative but no new emission bands are detected.[35] Moreover, it seems that the thienyl twisting is involved in the ICT population probability. This ring at the *meso* position contributes to the LUMO (see compound **5e** in Figure 3), as expected due to its rotational freedom (rotational barrier of 5.5 kcal/mol, less than that of **5a** due to the smaller thiophene ring, Figure 4), but what is more striking is the increase of the dihedral angle upon excitation (from 45 to 65°, Figure 3). Such a more perpendicular orientation of the thienyl group in the excited state is in agreement with a twisted ICT (TICT).[36]

Finally, it should be stressed that the photophysics of the BODIPY are not affected by the bulky fragment generated after MCR either at the *para* position of the 8-phenyl group or directly at the BODIPY 2-position since it is separated from the chromophoric core by a methine unit. Thus, the synthetic route reported herein is a cost-effective and straightforward method to design smart multichromophoric assemblies from BODIPYs or other fluorophores with the required functionality, in which each fragment retains its molecular identity.

Biological Assays. We have tested the ability of the 11 BODIPYs described herein to be used as possible probes for fluorescence microscopy using human phagocytic cells. First, we aimed to assess whether or not BODIPYs were suitable for tracking the fungal cell phagocytic processes in human-derived macrophages. After 3 h of *Candida parapsilosis*–macrophage interaction, BODIPYs were added and compounds **4b–e** and **5a–d** showed a fluorescent signal in the green channel; nevertheless, it was quenched soon afterward, independent of the concentration used. In all cases, BODIPYs showed affinity

DOI: 10.1021/acs.joc.5b02893
J. Org. Chem. 2016, 81, 2888–2898

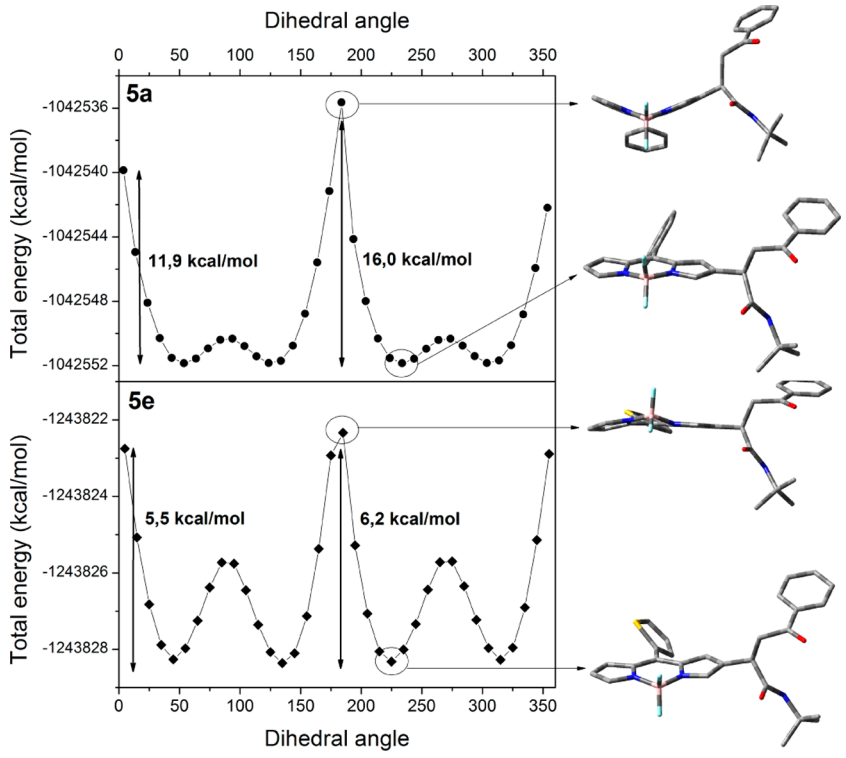

Figure 4. Computed energy surfaces for the rotation of the 8-phenyl (**5a**) and 8-thenyl (**5e**) derivatives with regard to the indacene plane in AcOEt. The corresponding geometries at the energy maximum and minimum are also shown.

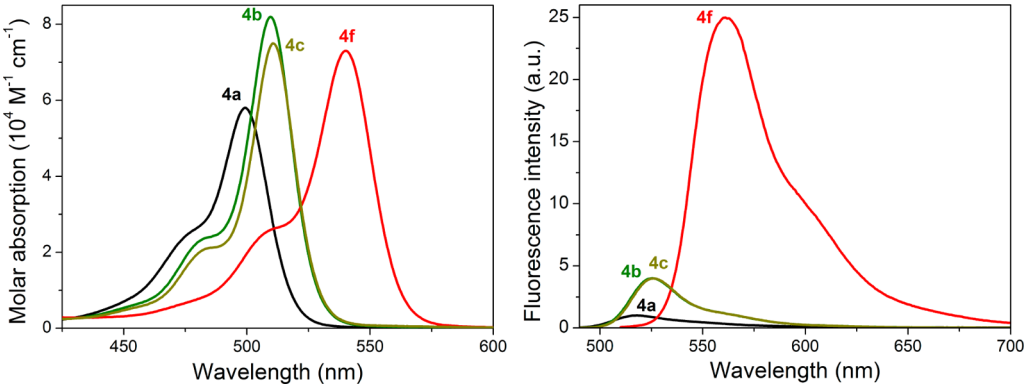

Figure 5. Absorption and fluorescence spectra of the compounds bearing unhindered 8-tolyl (**4a**), with alkyls at positions α (methyl **4b** and ethyl **4c**) and bromines at positions β (**4f**) in diluted solutions of ethyl acetate.

to small unidentified vesicles in the periphery of the macrophage but not to the phagolysosome, making the tracking of the phagocytic process infeasible (Figure 7). Acridine orange staining was used as a control to assess phagocytosis.[37]

Then, we further investigated the selectivity of the BODIPYs for different blood cells by staining monocytes, granulocytes, and erythrocytes with them. Fluorescence remained constant during the whole observation period for all compounds. Unlike the rest of the BODIPYs, compounds **4b** and **5b** preferentially stained the erythrocyte membrane, but the former caused cell crenation (Figure 8A–D). The rest of the compounds mostly stained the cytoplasm but not the nuclei of monocyte and granulocyte cells (Figure 8E–H). BODIPYs **4b** and **5b** exhibit an excellent performance at 75 ms of exposure, while the rest of the compounds worked better at 150 ms of exposure. The only exception was the BODIPY **4d** that needed 700 ms to achieve a defined signal.

CONCLUSIONS

We have described the synthesis of formyl-containing BODIPY derivatives using either the Liebeskind–Srogl cross-coupling reaction (six examples) or the Vilsmeier reaction (five examples). These dyes were used along with benzoic acid and *t*-butyl isocyanide in the Passerini reaction to produce 11 new dyes with rich functionality in a straightforward manner. The photophysical signatures of the formylated BODIPYs are ruled by the free motion of the 8-aryl and are kept after the MCR. Thus, this synthetic route is a straightforward method to design smart multichromophoric assemblies. These compounds are not suitable for phagocytosis tracking; nevertheless, some of them can be used as fluorescent agents to identify blood cells in a very efficient manner since fluorescence remains constant and intense at a very low exposure time. Other examples of MCR with formylBODIPYs as well as other formyl-containing fluorophores

DOI: 10.1021/acs.joc.5b02893
J. Org. Chem. 2016, 81, 2888–2898

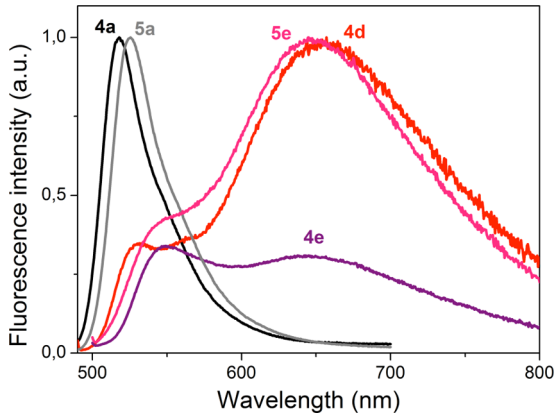

Figure 6. Fluorescence spectra of the compounds bearing 8-thienyl (**4d**,**e** and **5e**) and their corresponding analogues with 8-phenyl (**4a** and **5a**, respectively) in diluted solutions of ethyl acetate.

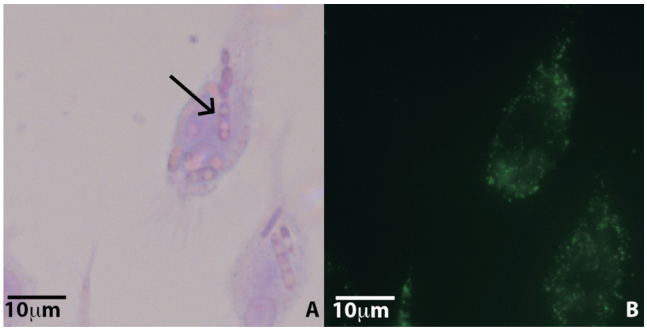

Figure 7. Phagocytosis assays in bright field (A) and fluorescence microscopy (B) using the BODIPY **5b**. The compound showed affinity to small unidentified vesicles in the macrophage but not to the phagolysosome, making the tracking of the phagocytic process infeasible. All compounds exhibited similar results.

are currently under investigation in our laboratories, and the results will be reported shortly.

EXPERIMENTAL SECTION

Synthesis and Characterization. Starting materials and reagents used in the preparation of BODIPYs are commercially available unless otherwise noted. The solvents were distilled and dried according to standard procedures before use. Unless stated otherwise, all reactions were performed without inert atmosphere in oven- or flame-dried glassware. Reaction progress was monitored by TLC (silica gel plates with an F-254 indicator), and the spots were visualized under UV light (254 or 365 nm). Flash column chromatography was performed using silica gel Kieselgel 60 (70−230 mesh) and a mixture of ethyl acetate and hexanes as the eluent. Spectral data of the known compounds were in accordance with the literature data. ^{1}H and ^{13}C NMR spectra were acquired on spectrometers (500 or 400 MHz for ^{1}H and 125 or 101 MHz for ^{13}C) in deuteriochloroform ($CDCl_3$) with either tetramethylsilane (TMS) (0.00 ppm ^{1}H, 0.00 ppm ^{13}C) or chloroform (7.26 ppm ^{1}H, 77.16 ppm ^{13}C) or as an internal reference unless otherwise stated.[38] Data are reported in the following order: chemical shifts in parts per million, multiplicities (br (broadened), s (singlet), d (doublet), t (triplet), q (quartet), sext (sextet), hept (heptet), m (multiplet), exch (exchangeable), app (apparent)), coupling constants J (Hz), and integration. Infrared spectra were recorded on a FTIR spectrophotometer. Peaks are reported (cm^{-1}) with the following relative intensities: s (strong, 67−100%), m (medium 40−66%), and w (weak 20−39%). Melting points were determined and were uncorrected. HRMS samples were ionized by ESI+ and recorded via the TOF method.

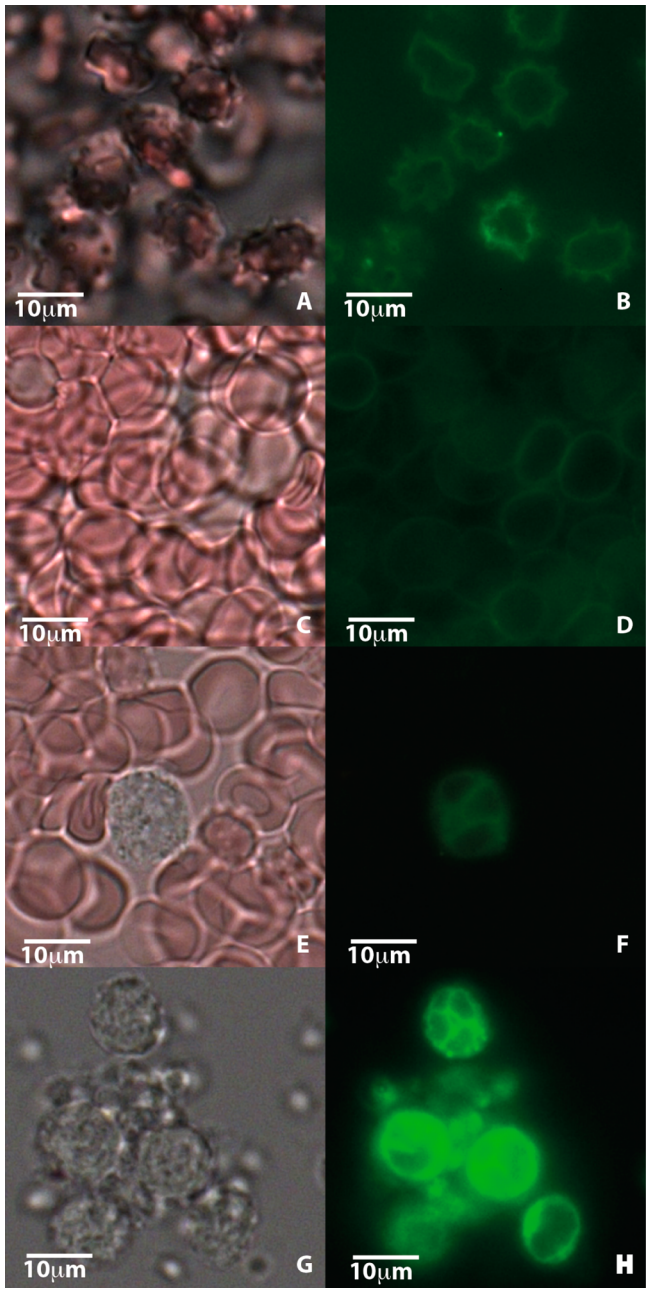

Figure 8. Compound **4b** stained the erythrocyte membrane, causing crenation of the cells (A,B) unlike compound **5b** that also stained the membrane of the red blood cells without crenation (C,D). Similarly, both compounds stained mononuclear cells in a similar way (G,H). The rest of them, as compound **4e**, selectively stained the granulocytes but not the erythrocytes (E,F), and all of them stained the mononuclear cells.

8-MethylthioBODIPYs **A**−**C**,[23] compounds **2a**−**c**, **3a**−**c**, **3e**,[39] and CuTC[40] were prepared according to the literature procedures.

Spectroscopic Measurements. The photophysical properties were registered in diluted solutions (around 2×10^{-6} M) of ethyl acetate, using quartz cuvettes with an optical pathway of 1 cm. UV−vis absorption and fluorescence spectra were recorded on a spectrophotometer and a spectrofluorimeter, respectively. Fluorescence quantum yield (ϕ) was obtained by using the commercial PM567 dye as the reference (ϕ^{r} = 0.84 in ethanol). Radiative decay curves were registered with the time-correlated single-photon counting technique, equipped with a microchannel plate detector of picosecond time resolution (20 ps). Fluorescence emission was monitored at the

DOI: 10.1021/acs.joc.5b02893
J. Org. Chem. 2016, 81, 2888−2898

maximum emission wavelength after excitation by means of a laser. The fluorescence lifetime (τ) was obtained after the deconvolution of the instrumental response signal from the recorded decay curves by means of an iterative method. The goodness of the exponential fit was controlled by statistical parameters (χ^2, Durbin-Watson and the analysis of the residuals). Radiative (k_{fl}) and nonradiative (k_{nr}) rate constants were calculated as follows; $k_{fl} = \phi/\tau$ and $k_{nr} = (1 - \phi)/\tau$.

Computational Modeling for Representative Compounds 5a, 5b, and 5e. Ground state energy minimizations were performed using Becke's three-paramater (B3LYP) density functional method, whereas excited state geometry optimization was carried out using the ab initio configuration interaction single method. The basis set was the double valence 6-31g* (with a polarization function). The optimized geometry was taken as a true energy minimum using frequency calculations (no negative frequencies). Rotational energy barriers in the ground state were calculated from the potential energy surface, which was simulated by relaxed scans (steps of 10°) of the 8-phenyl, 8-thienyl, and 8-mesityl twist with regard to the plane of the BODIPY core. The solvent effect (ethyl acetate) was considered in all calculations by the polarizable continuum model. All calculations were performed in Gaussian 09, using the "arina" computational resources provided by the UPV-EHU.

Biological Assays. Peripheral blood mononuclear cells were isolated from human blood as previously described.[41] The differentiation to macrophages was induced in serum-free medium supplemented with 1% (v/v) penicillin−streptomycin solution and 10 ng/mL recombinant human granulocyte−macrophage colony-stimulating factor, under incubation at 37 °C, 5% (v/v) CO_2 for 6−7 days, with the medium being replaced every 2−3 days.[42] Macrophage infection with *Candida parapsilosis* yeast cells was performed at a multiplicty of infection of 1:5, respectively. After 3 h of incubation at 37 °C, 5% (v/v) CO_2, cells were treated with the BODIPY at a final concentration of either 1 or 5 μg/mL in phosphate-buffered saline (PBS), pH 7.4, letting the compound interact for 5 min at room temperature. Cells were washed, and crystal violet solution (0.03% in PBS) was added for contrast. After 3 min, cells were washed again and placed onto slides to be inspected under a fluorescence microscope. For interaction of BODIPYs with monocytes, granulocytes, and erythrocytes, cells were suspended in PBS containing the BODIPY at a final concentration of 1 μg/mL. After 15 min of incubation at room temperature, cells were washed twice with PBS and placed onto slides for inspection under the fluorescence microscope.

All preparations were examined using a microscope. Acquisition of images was achieved by means of AxioVs40 V 4.6.1.0 software and a camera.

Synthesis and Characterization of Compounds. *General Procedure for the Liebeskind−Srogl Cross-Coupling Reaction (GP1).* An oven-dried Schlenk tube, equipped with a stir bar, was charged with 8-methylthioBODIPY **A** or **B** (1.0 equiv), the corresponding boronic acid (3.0 equiv), and dry THF (0.03 M) under N_2. The mixture was sparged with N_2 for 5 min, whereupon $Pd_2(dba)_3$ (2.5 mol %), trifurylphosphine (7.5 mol %), and CuTC (3.0 equiv) were added followed by a 5 min N_2 purge. The reaction mixture was immersed into a preheated oil bath at 55 °C. After TLC showed that the reaction went to completion, the reaction mixture was allowed to reach room temperature and was adsorbed on SiO_2 gel. After flash chromatography (SiO_2 gel, EtOAc/hexanes gradient) and purification, *meso*-substituted BODIPYs were obtained as highly colored solids.

General Procedure for the Synthesis of β-FormylBODIPYs (GP2). In a round-bottomed flask equipped with a stir bar, DMF (3.0 mL, 39 mmol) and $POCl_3$ (3.0 mL, 32 mmol) were combined at 0 °C (ice bath) under N_2 for 5 min. After being warmed to room temperature, the reaction mixture was further stirred for 30 min. Then, the corresponding 8-(het)arylBODIPY (0.2 mmol) in $ClCH_2CH_2Cl$ (10 mL) was added to the reaction mixture. After the temperature was increased to 80 °C, the reaction mixture was further stirred for 16 h, cooled to room temperature, and slowly poured into a saturated aqueous K_2CO_3 solution (100 mL) cooled in an ice bath. After being warmed to room temperature, the reaction mixture was further stirred for 1 h and extracted with CH_2Cl_2 (3 × 50 mL). The organic layers were combined, washed with water (2 × 50 mL), dried with anhydrous $MgSO_4$, and filtered, and the solvent was removed under reduced pressure. The crude product was further purified by column chromatography on silica gel using a mixture of ethyl acetate and hexanes as eluent to give the β-formylated BODIPYs as dark red crystals.

General Procedure for the Passerini Reaction (GP3). To a solution of corresponding formylBODIPY **2** or **3** (1.0 equiv) in dichloromethane (0.5 mL) were sequentially added benzoic acid (3.0 equiv) and *tert*-butyl isocyanide (3.0 equiv) at room temperature, followed by addition of H_2O (0.5 mL). The reaction mixture was stirred at room temperature for 24 h until completion (TLC monitoring). When the reaction was completed, the product was extracted with ethyl acetate, washed with brine (3 × 10 mL), dried with anhydrous $MgSO_4$, and filtered. The solvent was removed under reduced pressure, and the crude product was purified by silica gel column chromatography (EtOAc/hexane gradient) to obtain the desired product.

Liebeskind−Srogl Cross-Coupling Reaction (Scheme 1). *According to GP1.*

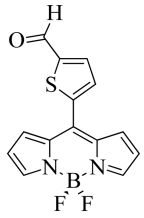

2d

A (70 mg, 0.2940 mmol, 1.0 equiv), 5-formyl-2-thienylboronic acid (138 mg, 0.8821 mmol, 3.0 equiv), CuTC (168 mg, 0.8821 mmol, 3.0 equiv), $Pd_2(dba)_3$ (6.7 mg, 0.0074 mmol, 2.5 mol %), and tri-2-furylphosphine (5.1 mg, 0.0220 mmol, 7.5 mol %). The desired product was obtained as a dark red crystals (69 mg, 78% yield): mp >150 °C (subl.); TLC (30% EtOAc/hexanes, R_f = 0.2); IR (KBr, cm^{-1}) 3111 (w), 3094 (w), 1672 (s), 1657 (s), 1548 (s), 1414 (s), 1386 (s), 1264 (s), 1212 (s), 1113 (s), 1076 (s), 969 (m), 776 (m), 666 (w), 630 (w), 583 (w); ^{1}H NMR (400 MHz, $CDCl_3$) δ 10.02 (s, 1H), 7.97 (s, 2H), 7.88 (d, J = 4.0 Hz, 1H), 7.58 (d, J = 4.0 Hz, 1H), 7.21 (d, J = 4.4 Hz, 2H), 6.60 (d, J = 4.0 Hz, 2H); ^{13}C NMR (101 MHz, $CDCl_3$) δ 182.9, 147.1, 145.6, 142.7, 137.5, 135.7, 134.4, 132.8, 131.6, 119.4; HRMS (ESI+) m/z calcd for $C_{14}H_{10}BF_2N_2OS$ $[M + H]^+$ 303.0572, found 303.0574.

According to GP1.

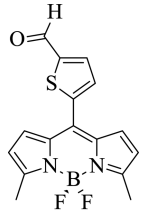

2e

B (80 mg, 0.3006 mmol, 1.0 equiv), 5-formyl-2-thienylboronic acid (141 mg, 0.9018 mmol, 3.0 equiv), CuTC (172 mg, 0.9018 mmol, 3.0 equiv), $Pd_2(dba)_3$ (6.9 mg, 0.0075 mmol, 2.5 mol %), and tri-2-furylphosphine (5.2 mg, 0.0225 mmol, 7.5 mol %). The desired product was obtained as a dark red crystals (86 mg, 87% yield): mp >180 °C (subl.); TLC (30% EtOAc/hexanes, R_f = 0.3); IR (KBr, cm^{-1}) 3111 (w), 2924 (w), 2852 (w), 1668 (s), 1552 (s), 1493 (s), 1457 (s), 1280 (s), 1211 (s), 1152 (s), 1012 (m), 817 (m), 729 (m), 675 (w); ^{1}H NMR (500 MHz, $CDCl_3$) δ 9.99 (s, 1H), 7.82 (d, J = 4.0 Hz, 1H), 7.46 (d, J = 3.5 Hz, 1H), 6.98 (d, J = 4.0 Hz, 2H), 6.32 (d, J = 4.0 Hz, 2H), 2.65 (s, 6H); ^{13}C NMR (126 MHz, $CDCl_3$) δ 182.8, 159.4, 146.1, 143.6, 135.6, 134.1, 132.7, 131.8, 130.3, 120.4, 15.2; HRMS (ESI+) m/z calcd for $C_{16}H_{14}BF_2N_2OS$ $[M + H]^+$ 331.0885, found 331.0886.

DOI: 10.1021/acs.joc.5b02893
J. Org. Chem. 2016, 81, 2888−2898

Synthesis of BODIPY 2f (Scheme 3). *BODIPY D.*

D

To a solution of **B** (50 mg, 0.1879 mmol, 1.0 equiv) in THF (3.0 mL) was added dropwise a solution of NBS (70 mg, 2.20 mmol, 2.1 equiv) in THF (1.5 mL) at room temperature. The mixture was stirred at room temperature for 1 h. The product was diluted with ethyl acetate (5.0 mL), washed with brine (2 × 10 mL), dried over $MgSO_4$, and filtered. The solvent was removed in vacuo to provide the desired product as a dark pink solid (74 mg, 93% yield): mp 109 °C; TLC (15% EtOAc/hexanes, R_f = 0.6); IR (KBr, cm^{-1}) 3540 (w), 2929 (w), 1739 (m), 1532 (m), 1450 (m), 1372 (m), 1314 (w), 1243 (s), 1174 (m), 1141 (s), 1090 (m), 1011 (m), 895 (m), 678 (w); ^1H NMR (200 MHz, $CDCl_3$) δ 7.43 (s, 2H), 2.82 (s, 3H), 2.6 (s, 6H); ^{13}C NMR (50 MHz, CD_3CN) δ 154.8, 145.6, 133.8, 128.3, 108.9, 21.7, 13.6; HRMS (ESI+) m/z calcd for $C_{12}H_{12}BBr_2F_2N_2S$ $[M + H]^+$ 424.9125, found 424.9121.

According to GP1.

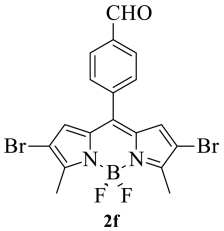

2f

D (100 mg, 0.2359 mmol, 1.0 equiv), 4-formylphenylboronic acid (88 mg, 0.5897 mmol, 2.5 equiv), CuTC (135 mg, 0.7077 mmol, 3.0 equiv), $Pd_2(dba)_3$ (5.4 mg, 0.0059 mmol, 2.5 mol %), and tri-2-furylphosphine (4.1 mg, 0.0018 mmol, 7.5 mol %). The desired product was obtained as dark purple crystals (102 mg, 90% yield): mp >210 °C (subl.); TLC (30% EtOAc/hexanes, R_f = 0.6); IR (KBr, cm^{-1}) 3122 (w), 2836 (w), 2737 (w), 1703 (s), 1575 (s), 1559 (s), 1452 (m), 1246 (s), 1130 (s), 1004 (m), 988 (m), 823 (m), 485 (m); ^1H NMR (500 MHz, $CDCl_3$) δ 10.13 (s, 1H), 8.03 (d, J = 8.0 Hz, 2H), 7.65 (d, J = 8.0 Hz, 2H), 6.74 (s, 2H), 2.64 (s, 6H); ^{13}C NMR (126 MHz, $CDCl_3$) δ 191.2, 157.0, 140.2, 139.0, 137.8, 133.0, 131.0, 130.3, 129.8, 109.7, 13.7; HRMS (ESI+) m/z calcd for $C_{18}H_{14}BBr_2F_2N_2O$ $[M + H]^+$ 482.9512, found 482.9506.

Synthesis of 2-FormylBODIPYs (Scheme 4). *According to GP2.*

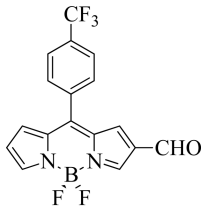

3d

DMF (3.0 mL, 39.0 mmol, 218.5 equiv), $POCl_3$ (3.0 mL, 32.0 mmol, 179.3 equiv), *p*-trifluoromethylphenylBODIPY (60 mg, 0.1785 mmol, 1.0 equiv), and DCE (20.0 mL). The desired product was obtained as a dark red crystals (26 mg, 40% yield): mp >210 °C (dec.); TLC (30% EtOAc/hexanes, R_f = 0.4); IR (KBr, cm^{-1}) 3109 (w), 2922 (m), 2851 (m), 1677 (s), 1544 (s), 1398 (s), 1329 (s), 1283 (m), 1171 (m), 1123 (m), 1098 (m), 976 (m), 915 (m), 855 (m), 740 (m), 718 (m), 649 (w); ^1H NMR (400 MHz, $CDCl_3$) δ 9.86 (s, 1H), 8.31 (s, 1H), 8.23 (s, 1H), 7.85 (d, J = 8.0 Hz, 2H), 7.72 (d, J = 8.0 Hz, 2H), 7.24 (s, 1H), 7.10 (d, J = 4.4 Hz, 1H), 6.76 (d, J = 4.4 Hz, 1H); ^{13}C NMR (101 MHz, $CDCl_3$) δ 184.8, 150.7, 147.4, 143.7, 137.1, 136.4, 134.7, 134.5, 133.6, 133.3, 132.2, 130.8, 128.7, 126.0 (q, $^3J_{CF}$ = 3.7 Hz), 125.0, 122.3; HRMS (ESI+) m/z calcd for $C_{17}H_{11}BF_5N_2O$ $[M + H]^+$ 365.0882, found 365.0897.

The Passerini Reaction (Scheme 5). *According to GP3.*

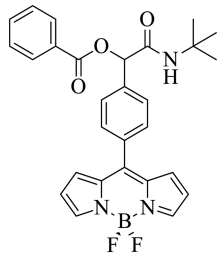

4a

2a (30 mg, 0.1013 mmol, 1.0 equiv), benzoic acid (37 mg, 0.3039 mmol, 3.0 equiv), and *tert*-butyl isocyanide (34.0 μL, 0.3039 mmol, 3.0 equiv) in CH_2Cl_2/H_2O (1:1, 1.0 mL). The desired product was obtained as a yellow solid (38 mg, 75% yield): mp 220–222 °C; TLC (30% EtOAc/hexanes, R_f = 0.3); IR (KBr, cm^{-1}) 3305 (m), 3079 (w), 2969 (w), 1727 (s), 1664 (s), 1556 (s), 1414 (s), 1387 (s), 1262 (s), 1112 (s), 1077 (s), 985 (w) 709 (m). ^1H NMR (500 MHz, $CDCl_3$) δ 8.13 (d, J = 7.5 Hz, 2H), 7.93 (s, 2H), 7.69 (d, J = 8.0 Hz, 2H), 7.65 (t, J = 7.5 Hz, 1H), 7.59 (d, J = 8.0 Hz, 2H), 7.53 (t, J = 7.8 Hz, 2H), 6.94 (d, J = 4.0 Hz, 2H), 6.53 (d, J = 3.0 Hz, 2H), 6.35 (s, 1H), 6.23 (br, 1H), 1.42 (s, 9H); ^{13}C NMR (126 MHz, $CDCl_3$) δ 167.0, 164.8, 146.7, 144.5, 139.0, 135.0, 134.4, 134.1, 131.8, 130.9, 129.9, 129.2, 129.0, 127.6, 118.8, 75.5, 52.0, 28.9; HRMS (ESI+) m/z calcd for $C_{28}H_{27}BF_2N_3O_3$ $[M + H]^+$ 502.2113, found 502.2112.

According to GP3.

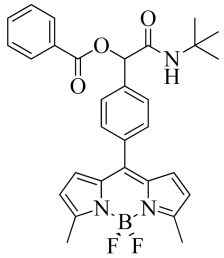

4b

2b (30 mg, 0.0926 mmol, 1.0 equiv), benzoic acid (34 mg, 0.2778 mmol, 3.0 equiv), and *tert*-butyl isocyanide (31.0 μL, 0.2778 mmol, 3.0 equiv) in CH_2Cl_2/H_2O (1:1, 1.0 mL). The desired product was obtained as an orange solid (43 mg, 87% yield): mp 201–203 °C; TLC (30% EtOAc/hexanes, R_f = 0.4); IR (KBr, cm^{-1}) 3299 (m), 3102 (w), 2969 (m), 1723 (s), 1666 (s), 1543 (s), 1413 (s), 1391 (s), 1259 (s), 1224 (s), 1080 (s), 973 (s), 839 (w), 767 (s), 758 (s), 718 (s); ^1H NMR (500 MHz, $CDCl_3$) δ 8.12 (d, J = 7.0 Hz, 2H), 7.66–7.63 (m, 3H), 7.53–7.50 (m, 4H), 6.71 (d, J = 4.0 Hz, 2H), 6.32 (s, 1H), 6.25 (d, J = 4.0 Hz, 2H), 6.19 (br, 1H), 2.64 (s, 6H), 1.41 (s, 9H); ^{13}C NMR (126 MHz, $CDCl_3$) δ 167.1, 164.9, 158.0, 141.8, 138.0, 134.8, 134.6, 134.0, 130.8, 130.6, 129.9, 129.3, 128.9, 127.4, 119.6, 75.6, 51.9, 28.9, 15.0; HRMS (ESI+) m/z calcd for $C_{30}H_{31}BF_2N_3O_3$ $[M + H]^+$ 530.2426, found 530.2429.

According to GP3.

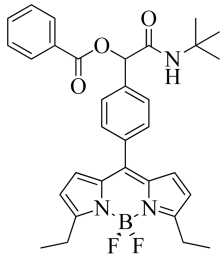

4c

2c (21 mg, 0.0596 mmol, 1.0 equiv), benzoic acid (22 mg, 0.1789 mmol, 3.0 equiv), and *tert*-butyl isocyanide (20.0 μL, 0.1789 mmol, 3.0 equiv) in CH_2Cl_2/H_2O (1:1, 1.0 mL). The desired product was obtained as an orange solid (30 mg, 90% yield): mp 166–168 °C; TLC (30% EtOAc/hexanes, R_f = 0.5); IR (KBr, cm^{-1}) 3305 (m), 2971(m), 2935 (w), 1725 (s), 1663 (s), 1555 (s), 1439 (s), 1319 (s), 1260 (s), 1141 (s), 1033 (s), 983 (m), 885 (m), 710 (s); ^1H NMR (500 MHz, $CDCl_3$)

DOI: 10.1021/acs.joc.5b02893
J. Org. Chem. 2016, 81, 2888–2898

δ 8.13 (d, J = 7.5 Hz, 2H), 7.66−7.63 (m, 3H), 7.54−7.51 (m, 4H), 6.74 (d, J = 4.0 Hz, 2H), 6.34−6.33 (m, 3H), 6.19 (br, 1H), 3.07 (q, J = 7.5 Hz, 4H), 1.42 (s, 9H), 1.34 (t, J = 7.6 Hz, 6H); ^{13}C NMR (126 MHz, $CDCl_3$) δ 167.1, 164.9, 163.9, 142.2, 138.0, 134.9, 134.3, 134.0, 130.8, 130.6, 129.9, 129.3, 129.0, 127.4, 117.5, 75.6, 51.9, 28.9, 22.2, 12.9; HRMS (ESI+) m/z calcd for $C_{32}H_{35}BF_2N_3O_3$ $[M + H]^+$, 558.2740; found 558.2738.

According to GP3.

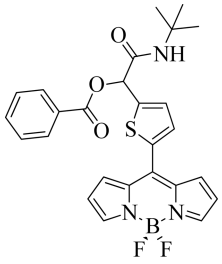

4d

2d (20 mg, 0.0662 mmol, 1.0 equiv), benzoic acid (24 mg, 0.1986 mmol, 3.0 equiv), and *tert*-butyl isocyanide (23 μL, 0.1986 mmol, 3.0 equiv) in CH_2Cl_2/H_2O (1:1, 1.0 mL). The desired product was obtained as a red solid (30 mg, 89% yield): mp 183−186 °C; TLC (30% EtOAc/hexanes, R_f = 0.3); IR (KBr, cm^{-1}) 3299 (m), 3102 (w), 2969 (m), 1723 (s), 1666 (s), 1543 (s), 1413 (s), 1391 (s), 1259 (s), 1080 (s), 973 (s), 767 (s), 718 (s); ^{1}H NMR (500 MHz, $CDCl_3$) δ 8.12 (d, J = 7.0 Hz, 2H), 7.92 (s, 2H), 7.66 (t, J = 7.5 Hz, 1H), 7.53 (t, J = 7.8 Hz, 2H), 7.45 (d, J = 4.0 Hz, 1H), 7.36 (d, J = 4.0 Hz, 1H), 7.27 (d, J = 4.0 Hz, 2H), 6.56 (m, 3H), 6.18 (br, 1H), 1.43 (s, 9H); ^{13}C NMR (126 MHz, $CDCl_3$) δ 165.8, 164.8, 144.3, 144.2, 139.0, 135.7, 134.4, 134.3, 132.7, 131.7, 130.0, 129.0, 128.8, 128.3, 118.8, 71.7, 52.2, 28.8; HRMS (ESI+) m/z calcd for $C_{26}H_{25}BF_2N_3O_3S$ $[M + H]^+$ 508.1677, found 508.1671.

According to GP3.

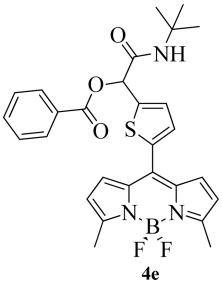

4e

2e (30 mg, 0.0908 mmol, 1.0 equiv), benzoic acid (33 mg, 0.2726 mmol, 3.0 equiv), and *tert*-butyl isocyanide (31.0 μL, 0.2726 mmol, 3.0 equiv) in CH_2Cl_2/H_2O (1:1, 1.0 mL). The desired product was obtained as a red solid (37 mg, 76% yield): mp 210−213 °C; TLC (30% EtOAc/hexanes, R_f = 0.4); IR (KBr, cm^{-1}) 3278 (m), 3086 (w), 2966 (m), 2918 (m), 2850 (w), 1722 (s), 1665 (s), 1556 (s), 1492 (s), 1452 (s), 1275 (s), 1143 (s), 1090 (m), 1014 (s), 975 (s), 796 (s), 710 (s); ^{1}H NMR (500 MHz, $CDCl_3$) δ 8.11 (d, J = 7.5 Hz, 2H), 7.65 (t, J = 7.4 Hz, 1H), 7.52 (t, J = 7.8 Hz, 2H), 7.32−7.30 (m, 2H), 7.05 (d, J = 4.0 Hz, 2H), 6.53 (s, 1H), 6.29 (d, J = 4.0 Hz, 2H), 6.13 (br, 1H), 2.64 (s, 6H), 1.42 (s, 9H); ^{13}C NMR (126 MHz, $CDCl_3$) δ 166.0, 164.8, 158.2, 142.3, 136.0, 134.3, 134.2, 131.4, 130.6, 130.0, 129.0, 128.6, 128.0, 119.7, 71.8, 52.1, 28.8, 15.1; HRMS (ESI+) m/z calcd for $C_{28}H_{29}BF_2N_3O_3S$ $[M + H]^+$ 536.1990, found 536.1992.

According to GP3.

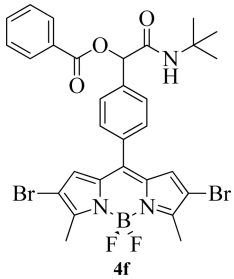

4f

2f (30 mg, 0.0622 mmol, 1.0 equiv), benzoic acid (23 mg, 0.1866 mmol, 3.0 equiv), and *tert*-butyl isocyanide (21.0 μL, 0.1866 mmol, 3.0 equiv) in CH_2Cl_2/H_2O (1:1, 1.0 mL). The desired product was obtained as a fuchsia solid (36 mg, 84% yield): mp >280 °C (subl.); TLC (30% EtOAc/hexanes, R_f = 0.6); IR (KBr, cm^{-1}) 3433 (w), 3120 (w), 2967 (w), 1733(s), 1684 (s), 1546 (s), 1451 (s), 1246 (s), 1146 (s), 1011 (s), 715 (m), 489 (m); ^{1}H NMR (500 MHz, $CDCl_3$) δ 8.13 (d, J = 7.0 Hz, 2H), 7.68−7.64 (m, 3H), 7.53 (t, J = 7.8 Hz, 2H), 7.49 (d, J = 8.5 Hz, 2H), 6.81 (s, 2H), 6.33 (s, 1H), 6.23 (br, 1H), 2.62 (s, 6H), 1.42 (s, 9H); ^{13}C NMR (126 MHz, $CDCl_3$) δ 166.9, 164.8, 156.2, 141.6, 138.9, 134.1, 133.7, 133.2, 130.7, 130.6, 129.9, 129.2, 129.0, 127.7, 109.2, 75.5, 52.0, 28.9, 13.6; HRMS (ESI+) m/z calcd for $C_{30}H_{29}BBr_2F_2N_3O_3$ $[M + H]^+$ 686.0618, found 686.0617.

According to GP3.

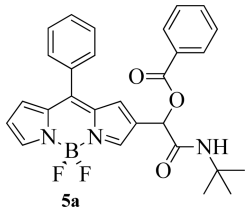

5a

3a (29 mg, 0.0979 mmol, 1.0 equiv), benzoic acid (36 mg, 0.2937 mmol, 3.0 equiv), and *tert*-butyl isocyanide (33.0 μL, 0.2937 mmol, 3.0 equiv) in CH_2Cl_2/H_2O (1:1, 1.0 mL). The desired product was obtained as an orange solid (33 mg, 68% yield): mp 172−174 °C; TLC (30% EtOAc/hexanes, R_f = 0.3); IR (KBr, cm^{-1}) 3394 (w), 2969 (w), 1717 (s), 1687 (s), 1552 (s), 1384 (m), 1259 (s), 1096 (s), 979 (w), 725 (w), 716 (w); ^{1}H NMR (400 MHz, $CDCl_3$) δ 8.06 (d, J = 7.2 Hz, 2H), 7.99 (d, J = 4.4 Hz, 2H), 7.64−7.45 (m, 8 H), 7.04 (s, 1H), 6.98 (d, J = 4.4 Hz, 1H), 6.58 (d, J = 3.2 Hz, 1H), 6.23 (s, 1H), 6.04 (br, 1H), 1.36 (s, 9H); ^{13}C NMR (101 MHz, $CDCl_3$) δ 166.8, 165.0, 148.2, 145.7, 141.6, 135.6, 134.6, 134.0, 133.8, 133.6, 132.8, 131.2, 130.7, 130.3, 129.9, 129.1, 128.9, 128.7, 128.6, 119.4, 70.2, 51.8, 28.8; HRMS (ESI+) m/z calcd for $C_{28}H_{26}BF_2N_3O_3Na$ $[M + Na]^+$ 524.1932, found 524.1934.

According to GP3.

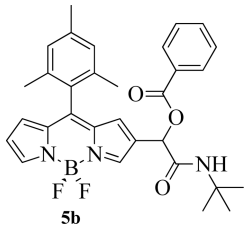

5b

3b (30 mg, 0.0887 mmol, 1.0 equiv), benzoic acid (33 mg, 0.2661 mmol, 3.0 equiv), and *tert*-butyl isocyanide (30.0 μL, 0.2661 mmol, 3.0 equiv) in CH_2Cl_2/H_2O (1:1, 1.0 mL). The desired product was obtained as a yellow solid (44 mg, 91% yield): mp 117−120 °C; TLC (30% EtOAc/hexanes, R_f = 0.5); IR (KBr, cm^{-1}) 3403 (w), 2973 (w), 2921 (w), 1721 (m), 1694 (m), 1563 (s), 1386 (m), 1364 (m), 1258 (s), 1104 (s), 1069 (m), 706 (m); ^{1}H NMR (500 MHz, $CDCl_3$) δ 8.06 (d, J = 7.0 Hz, 2H), 7.95 (s, 2H), 7.62 (t, J = 7.4 Hz, 1H), 7.49 (t, J = 7.7 Hz, 2H), 6.94 (s, 2H), 6.78 (s, 1H), 6.73 (d, J = 4.0 Hz, 1H), 6.50 (d, J = 3.5 Hz, 1H), 6.15 (s, 1H), 5.91 (br, 1H), 2.36 (s, 3H), 2.09 (s, 3H), 2.08 (s, 3H), 1.34 (s, 9H); ^{13}C NMR (126 MHz, $CDCl_3$) δ 166.8,165.0, 148.7, 145.9, 141.8, 139.2, 136.4, 136.3, 136.2, 135.1, 133.9, 131.4, 130.0, 129.5, 129.2,128.9, 128.5, 128.4, 128.3, 119.4, 70.3, 51.8, 28.8, 21.2, 20.2, 20.1; HRMS (ESI+) m/z calcd for $C_{31}H_{32}BF_2N_3O_3Na$ $[M + Na]^+$ 566.2402, found 566.2405.

According to GP3.

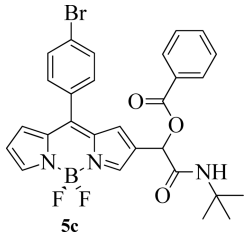

5c

3c (15 mg, 0.0400 mmol, 1.0 equiv), benzoic acid (15 mg, 0.1200 mmol, 3.0 equiv), and *tert*-butyl isocyanide (14.0 μL, 0.1200 mmol, 3.0 equiv)

DOI: 10.1021/acs.joc.5b02893
J. Org. Chem. 2016, 81, 2888−2898

in CH_2Cl_2/H_2O (1:1, 1.0 mL). The desired product was obtained as an orange solid (9 mg, 40% yield): mp 108−110 °C; TLC (30% EtOAc/hexanes, R_f = 0.4); IR (KBr, cm^{-1}) 3400 (w), 2968 (w), 1724 (m), 1692 (m), 1570 (s), 1545 (m), 1385 (m), 1364 (m), 1258 (s), 1101 (s), 912 (w), 711 (w); ^1H NMR (500 MHz, $CDCl_3$) δ 8.06 (d, J = 7.5 Hz, 2H), 7.99 (s, 2H), 7.68 (d, J = 8.0 Hz, 2H), 7.63 (t, J = 7.4 Hz, 1H), 7.50 (t, J = 7.6 Hz, 2H), 7.44 (d, J = 8.5 Hz, 2H), 7.01 (s, 1H), 6.94 (d, J = 3 5 Hz, 1H), 6.59 (d, J = 3.5 Hz, 1H), 6.22 (s, 1H), 6.02 (br, 1H), 1.37 (s, 9H); ^{13}C NMR (126 MHz, $CDCl_3$) δ 166.7, 165.0, 146.6, 146.1, 142.2, 135.4, 134.4, 134.0, 132.5, 132.4, 132.1, 132.0, 129.9, 129.6, 129.2, 128.9, 126.0, 119.6, 70.2, 51.9, 28.8; HRMS (ESI+) m/z calcd for $C_{28}H_{25}BBrF_2N_3O_3Na$ $[M + Na]^+$ 602.1038, found 602.1041.

According to GP3.

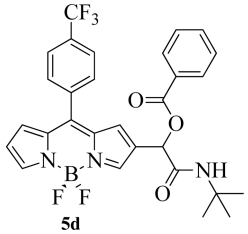

5d

3d (20 mg, 0.0549 mmol, 1.0 equiv), benzoic acid (20 mg, 0.1648 mmol, 3.0 equiv), and *tert*-butyl isocyanide (19.0 μL, 0.1648 mmol, 3.0 equiv) in CH_2Cl_2/H_2O (1:1, 1.0 mL). The desired product was obtained as an orange solid (12 mg, 38% yield): mp 193−196 °C; TLC (30% EtOAc/hexanes, R_f = 0.5); IR (KBr, cm^{-1}) 3393 (w), 2968 (w), 1723 (m), 1681 (m), 1553 (s), 1325 (m), 1258 (s), 1100 (s), 915 (w), 715 (m); ^1H NMR (500 MHz, $CDCl_3$) δ 8.06 (d, J = 7.5 Hz, 2H), 8.02 (s, 2H), 7.80 (d, J = 8.0 Hz, 2H), 7.69 (d, J = 8.0 Hz, 2H), 6.63 (t, J = 7.5 Hz, 1H), 7.50 (t, J = 7.8 Hz, 2H), 6.97 (s, 1H), 6.91 (d, J = 4.0 Hz, 1H), 6.60 (d, J = 3.5 Hz, 1H), 6.22 (s, 1H), 6.04 (br, 1H), 1.36 (s, 9H); ^{13}C NMR (126 MHz, $CDCl_3$) δ 166.6, 165.0, 146.6, 145.9, 142.6, 137.0, 135.5, 134.5, 134.0, 132.4, 130.8, 129.9, 129.6, 129.1, 129.0, 125.8, 125.7, 124.9, 119.9, 70.1, 51.9, 28.8; HRMS (ESI+) m/z calcd for $C_{29}H_{25}BF_5N_3O_3Na$ $[M + Na]^+$ 592.1806, found 592.1807.

According to GP3.

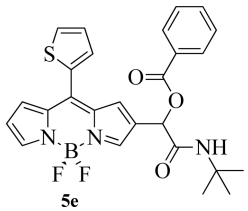

5e

3e (15 mg, 0.0500 mmol, 1.0 equiv), benzoic acid (18 mg, 0.1500 mmol, 3.0 equiv), and *tert*-butyl isocyanide (17.0 μL, 0.1500 mmol, 3.0 equiv) in CH_2Cl_2/H_2O (1:1, 1.0 mL). The desired product was obtained as a red solid (15 mg, 60% yield): mp >60 °C (dec.); TLC (30% EtOAc/hexanes, R_f = 0.3); IR (KBr, cm^{-1}) 3400 (w), 2965 (w), 1723 (m), 1682 (m), 1546 (s), 1409 (s), 1388 (s), 1260 (s), 1105 (s), 975 (w), 711 (m); ^1H NMR (500 MHz, $CDCl_3$) δ 8.07 (d, J = 8.0 Hz, 2H), 7.97 (s, 2H), 7.73 (d, J = 5.0 Hz, 1H), 7.63 (t, J = 7.2 Hz, 1H), 7.58 (d, J = 3.5 Hz, 1H), 7.49 (t, J = 7.6 Hz, 2H), 7.38 (s, 1H), 7.32 (d, J = 3.5 Hz, 1H), 7.28 (d, J = 4.0 Hz, 1H), 6.61 (d, J = 3.5 Hz, 1 H), 6.25 (s, 1H), 6.03 (br, 1H), 1.38 (s, 9H); ^{13}C NMR (126 MHz, $CDCl_3$) δ 166.8, 165.0, 145.3, 141.4, 140.4, 135.0, 134.5, 134.0, 133.6, 132.6, 132.1, 130.0, 129.8, 129.2, 128.9, 128.6, 119.3, 51.9, 28.8; HRMS (ESI+) m/z calcd for $C_{26}H_{24}BF_2N_3O_3SNa$ $[M + Na]^+$ 530.1496, found 530.1501.

■ ASSOCIATED CONTENT

Supporting Information

The Supporting Information is available free of charge on the ACS Publications website at DOI: 10.1021/acs.joc.5b02893.

Copies of ^1H and ^{13}C NMR spectra of all compounds in this paper and numerical documentation of the theoretical calculations (PDF)

■ AUTHOR INFORMATION

Corresponding Authors

*E-mail: jorge.banuelos@ehu.es.

*E-mail: eduardop@ugto.mx.

Notes

The authors declare no competing financial interest.

■ ACKNOWLEDGMENTS

Financial support from the MINECO (MAT2014-51937-C3-03) and Gobierno Vasco (IT339-10 and IT912-16) of Spain are thanked. D.E.R.-O. and E.A.-M. thank CONACyT for a graduate scholarship. We thank CONACyT (Grants 129572, 123732, CB2011-166860, and PN2014-247109) for financial support. L.A.P.-G. and H.M.M.-M. thank Sociedad Latinoamericana de Glicobiología A.C. and Universidad de Guanajuato (Grant DAIP-529/2015). Donation of Biellman BODIPYs by Cuantico de Mexico (www.cuantico.mx) is kindly appreciated.

■ REFERENCES

(1) (a) Dömling, A.; Wang, W.; Wang, K. *Chem. Rev.* **2012**, *112*, 3083. (b) Dömling, A. *Chem. Rev.* **2006**, *106*, 17. (c) Shestopalov, A. M.; Shestopalov, A. A.; Rodinovskaya, L. A. *Synthesis* **2008**, *2008*, 1. (d) Weber, L.; Illgen, K.; Almstetter, M. *Synlett* **1999**, *1999*, 366. (e) Zhu, J. *Eur. J. Org. Chem.* **2003**, *2003*, 1133. (f) Dömling, A.; Ugi, I. *Angew. Chem., Int. Ed.* **2000**, *39*, 3168.

(2) Martinez-Ariza, G.; Ayaz, M.; Medda, F.; Hulme, C. *J. Org. Chem.* **2014**, *79*, 5153.

(3) Siddiqui, I. R.; Rai, P.; Srivastava, A.; Shamim, S. *Tetrahedron Lett.* **2014**, *55*, 1159.

(4) Lv, L.; Zheng, S.; Cai, X.; Chen, Z.; Zhu, Q.; Liu, S. *ACS Comb. Sci.* **2013**, *15*, 183.

(5) Soleimani, E.; Ghorbani, S.; Ghasempour, H. R. *Tetrahedron* **2013**, *69*, 8511.

(6) Cai, Z.-J.; Wang, S.-Y.; Ji, S.-J. *Org. Lett.* **2012**, *14*, 6068.

(7) Wang, W.; Dömling, A. *J. Comb. Chem.* **2009**, *11*, 403.

(8) Zhou, H.; Zhang, W.; Yan, B. *J. Comb. Chem.* **2010**, *12*, 206.

(9) Rhoden, C. R. B.; Rivera, D. G.; Kreye, O.; Bauer, A. K.; Westermann, B.; Wessjohann, L. A. *J. Comb. Chem.* **2009**, *11*, 1078.

(10) Sachdeva, H.; Dwivedi, D. *Sci. World J.* **2012**, *2012*, 1.

(11) Vijesh, A. M.; Isloor, A. M.; Peethambar, S. K.; Shivananda, K. N.; Arulmoli, T.; Isloor, N. A. *Eur. J. Med. Chem.* **2011**, *46*, 5591.

(12) Chan, C. Y. K.; Tseng, N.-W.; Lam, J. W.Y.; Liu, J.; Kwok, R. T. K.; Tang, B. Z. *Macromolecules* **2013**, *46*, 3246.

(13) Padmaja, P.; Rao, G. K.; Indrasena, A.; Reddy, B. V. S.; Patel, N.; Shaik, A. B.; Reddy, N.; Dubey, P. K.; Bhadra, M. P. *Org. Biomol. Chem.* **2015**, *13*, 1404.

(14) (a) Hayek, A.; Bolze, F.; Bourgogne, C.; Baldeck, P. L.; Didier, P.; Arntz, Y.; Mély, Y.; Nicoud, J.-F. *Inorg. Chem.* **2009**, *48*, 9112. (b) Lin, W.; Long, L.; Tan, W. *Chem. Commun.* **2010**, *46*, 1503. (c) de Silva, A. P.; Vance, T. P.; West, M. E. S.; Wright, G. D. *Org. Biomol. Chem.* **2008**, *6*, 2468. (d) Lavis, L. D.; Raines, R. T. *ACS Chem. Biol.* **2008**, *3*, 142.

(15) (a) Cui, S.-L.; Lin, X.-F.; Wang, Y.-G. *J. Org. Chem.* **2005**, *70*, 2866. (b) Cui, S.-L.; Lin, X.-F.; Wang, Y.-G. *Org. Lett.* **2006**, *8*, 4517.

(16) Burchak, O. N.; Mugherli, L.; Ostuni, M.; Lacapere, J. J.; Balakirev, M. Y. *J. Am. Chem. Soc.* **2011**, *133*, 10058.

(17) Rotaru, A. V.; Druta, I. D.; Oeser, T.; Müller, T. J. J. *Helv. Chim. Acta* **2005**, *88*, 1798.

(18) Vázquez-Romero, A.; Kielland, N.; Arévalo, M. J.; Preciado, S.; Mellanby, R. J.; Feng, Y.; Lavilla, R.; Vendrell, M. *J. Am. Chem. Soc.* **2013**, *135*, 16018.

(19) Haugland, R. P. *The Handbook: A Guide to Fluorescent Probes and Labeling Technologies*, 10th ed.; Molecular Probes Inc.: Eugene, OR, 2005.

(20) Banfi, L.; Riva, R. *Org. React.* **2005**, *65*, 1.

(21) Bienaymé, H.; Bouzid, K. *Angew. Chem., Int. Ed.* **1998**, *37*, 2234.

DOI: 10.1021/acs.joc.5b02893
J. Org. Chem. 2016, 81, 2888−2898

(22) Ugi, I.; Steinbruckner, C. *Angew. Chem.* **1960**, *72*, 267.
(23) Alternatively, **A**−**C** can be prepared according to: Goud, T. V.; Tutar, A.; Biellmann, J.-F. *Tetrahedron* **2006**, *62*, 5084.
(24) (a) Peña-Cabrera, E.; Aguilar-Aguilar, A.; Gonzalez-Dominguez, M.; Lager, E.; Zamudio-Vazquez, R.; Godoy-Vargas, J.; Villanueva-García, F. *Org. Lett.* **2007**, *9*, 3985. (b) Betancourt-Mendiola, L.; Valois-Escamilla, I.; Arbeloa, T.; Bañuelos, J.; López Arbeloa, I.; Flores-Rizo, J. O.; Hu, R.; Lager, E.; Gómez-Durán, C. F. A.; Belmonte-Vázquez, J. L.; Martínez-González, M. R.; Arroyo, I. J.; Osorio-Martínez, C. A.; Alvarado-Martínez, E.; Urías-Benavides, A.; Gutiérrez-Ramos, B. D.; Tang, B. Z.; Peña-Cabrera, E. *J. Org. Chem.* **2015**, *80*, 5771.
(25) (a) Jiao, L.; Yu, C.; Li, J.; Wang, Z.; Wu, M.; Hao, E. *J. Org. Chem.* **2009**, *74*, 7525. (b) Zhang, J.; Zhu, S.; Valenzano, L.; Luo, F.-T.; Liu, H. *RSC Adv.* **2013**, *3*, 68. (c) Zhu, S.; Bi, J.; Vegesna, G.; Zhang, J.; Luo, F.-T.; Valenzano, L.; Liu, H. *RSC Adv.* **2013**, *3*, 4793.
(26) Gómez-Durán, C. F. A.; Esnal, I.; Valois-Escamilla, I.; Urías-Benavides, A.; Bañuelos, J.; López Arbeloa, I.; García-Moreno, I.; Peña-Cabrera, E. *Chem. - Eur. J.* **2016**, *22*, 1048.
(27) (a) Li, F.; Yang, S. I.; Ciringh, Y.; Seth, J.; Martin, C. H., III; Singh, D. L.; Kim, D.; Birge, R. R.; Bocian, D. F.; Holten, D.; Lindsey, J. S. *J. Am. Chem. Soc.* **1998**, *120*, 10001. (b) Kee, H. L.; Kirmaier, C.; Yu, L.; Thamyongkit, P.; Youngblood, W. J.; Calder, M. E.; Ramos, L.; Noll, B. C.; Bocian, D. F.; Scheidt, W. R.; Birge, R. R.; Lindsey, J. S.; Holten, D. *J. Phys. Chem. B* **2005**, *109*, 20433. (c) Alamiry, M. A. H.; Benniston, A. C.; Copley, G.; Elliott, K. J.; Harriman, A.; Stewart, B.; Zhi, Y. G. *Chem. Mater.* **2008**, *20*, 4024.
(28) (a) Badre, S.; Monnier, V.; Meallet-Renault, R.; Dumas-Verdes, C.; Schmidt, E. Y.; Mikhaleva, A.; Laurent, G.; Levi, G.; Ibañez, A.; Trofimov, B. A.; Pansu, R. B. *J. Photochem. Photobiol., A* **2006**, *183*, 238. (b) Zheng, Q.; Xu, G.; Prasad, P. N. *Chem. - Eur. J.* **2008**, *14*, 5812.
(29) (a) Cui, A.; Peng, X.; Fan, J.; Chen, X.; Wu, Y.; Guo, B. *J. Photochem. Photobiol., A* **2007**, *186*, 85. (b) Mukherjee, S.; Thilagar, P. *RSC Adv.* **2015**, *5*, 2706.
(30) (a) Sabatini, R. P.; McCormick, T. M.; Lazarides, T.; Wilson, K. C.; Eisenberg, R.; McCamant, D. W. *J. Phys. Chem. Lett.* **2011**, *2*, 223. (b) Lakshmi, V.; Ravikanth, M. *Dalton Trans.* **2012**, *41*, 5903. (c) Zhang, X. F.; Yang, X.; Niu, K.; Geng, H. *J. Photochem. Photobiol., A* **2014**, *285*, 16.
(31) Durán-Sampedro, G.; Agarrabeitia, A. R.; García-Moreno, I.; Costela, A.; Bañuelos, J.; Arbeloa, T.; López Arbeloa, I.; Chiara, J. L.; Ortiz, M. J. *Eur, J. Org. Chem.* **2012**, *2012*, 6335.
(32) (a) Chen, Y.; Zhao, J.; Guo, H.; Xie, L. *J. Org. Chem.* **2012**, *77*, 2192. (b) Poirel, A.; De Nicola, A.; Ziessel, R. *Org. Lett.* **2012**, *14*, 5696. (c) Yang, Y.; Guo, Q.; Chen, H.; Zhou, Z.; Guo, Z.; Shen, Z. *Chem. Commun.* **2013**, *49*, 3940.
(33) (a) Kim, K.; Jo, C.; Easwaramoorthi, S.; Sung, J.; Kim, D. H.; Churchill, D. G. *Inorg. Chem.* **2010**, *49*, 4881. (b) Collado, D.; Casado, J.; Rodriguez Gonzalez, S.; López Navarrete, J. T.; Suau, R.; Pérez-Inestrosa, E.; Pappenfus, T. M.; Raposo, M. M. M. *Chem. - Eur. J.* **2011**, *17*, 498.
(34) Benniston, A. C.; Clift, S.; Hagon, J.; Lemmetyinen, H.; Tkachenko, N. V.; Clegg, W.; Harrington, R. W. *ChemPhysChem* **2012**, *13*, 3672.
(35) Cunha Dias de Rezende, L.; Menezes Vaidergorn, M.; Biazzotto Moraes, J. C.; Da Silva Emery, F. *J. Fluoresc.* **2014**, *24*, 257.
(36) Grabowski, Z. R.; Rotkiewicz; Rettig, W. *Chem. Rev.* **2003**, *103*, 3899.
(37) Pruzanski, W.; Saito, S. *Inflammation* **1988**, *12*, 87.
(38) Gottlieb, H. E.; Kotlyar, V.; Nudelman, A. *J. Org. Chem.* **1997**, *62*, 7512.
(39) (a) For compound **2a**, see ref 24a. (b) Miao, Q.; Shin, J. Y.; Patrick, B. O.; Dolphin, D. *Chem. Commun.* **2009**, 2541 (for compound **2b**). (c) For compound **2c**, see ref 24b. (d) Melanson, J. A.; Smithen, D. A.; Cameron, S. T.; Thompson, A. *Can. J. Chem.* **2014**, *92*, 688. (e) Kee, H. L.; Kirmaier, C.; Yu, L.; Thamyongkit, P.; Youngblood, W. J.; Calder, M. E.; Ramos, L.; Noll, B. C.; Bocian, D. F.; Scheidt, W. R.; Birge, R. R.; Lindsey, J. S.; Holten, D. *J. Phys. Chem. B* **2005**, *109*, 20433. (f) Yu, C.; Jiao, L.; Yin, H.; Zhou, J.; Pang, W.; Wu, Y.; Wang, Z.; Yang, G.; Hao, E. *Eur. J. Org. Chem.* **2011**, *2011*, 5460 (for compounds **3a**−**c** and **3e**).
(40) Zhang, S.; Zhang, D.; Liebeskind, L. S. *J. Org. Chem.* **1997**, *62*, 2312. Cu(I)TC is also commercially available.
(41) Endres, S.; Ghorbani, R.; Lonnemann, G.; van der Meer, J. W.; Dinarello, C. A. *Clin. Immunol. Immunopathol.* **1988**, *49*, 424.
(42) Netea, M. G.; Nold-Petry, C. A.; Nold, M. F.; Joosten, L. A. B.; Opitz, B.; van der Meer, J. H. M.; van de Veerdonk, F. L.; Ferwerda, G.; Heinhuis, B.; Devesa, I.; Funk, C. J.; Mason, R. J.; Kullberg, B. J.; Rubartelli, A.; van der Meer, J. W. M.; Dinarello, C. A. *Blood* **2009**, *113*, 2324.

DOI: 10.1021/acs.joc.5b02893
J. Org. Chem. 2016, 81, 2888−2898